JOURNAL OF SOLID STATE CHEMISTRY **132,** 399–406 (1997)
ARTICLE NO. SC977485

Interaction of Silver Ions in Solution with Copper Hexacyanoferrate (II) $Cu_2Fe(CN)_6$

F. Adekola,* M. Fedoroff,*,[1] S. Ayrault,† C. Loos-Neskovic,† E. Garnier,‡ and L.-T. Yu§

* *Centre National de la Recherche Scientifique, Centre d'Etudes de Chimie Métallurgique, 15, rue Georges Urbain, 94407 Vitry-sur-Seine, France;* † *Laboratoire P. Süe, C. E. N. Saclay, 91191 Gif-sur-Yvette, France;* ‡ *Laboratoire de Chimie Théorique, Université de Poitiers, 40, Avenue du Recteur Pineau, 86022 Poitiers, France; and* § *Laboratoire d'Electrochimie, Catalyse et Synthèse Organique, 2, rue Henri Dunant, 94320 Thiais, France*

Received January 14, 1997; in revised form May 19, 1997; accepted May 22, 1997

The sorption of silver ions from 0.1 *M* HNO_3 solutions on copper hexacyanoferrate (II) $Cu_2^{II}Fe^{II}(CN)_6$ was investigated using batch experiments. Sorption kinetics and isotherms were studied in which ICP/AES was used for determining the amount of sorbed Ag and the quantities of elements released into the solution. Cyclic voltammetry and X-ray diffraction were used for determining the evolution of the solid. This hexacyanoferrate is very efficient for the removal of silver from aqueous solutions: more than 99.999% of the silver can be removed for initial concentrations less than 0.01 mol/l. Silver sorption proceeds with fast kinetics in a first step and with a further slow evolution. The sorption capacity reaches 1.4 g Ag per g of sorbent. The sorption mechanism is rather complex: there is a destruction of the initial crystalline structure along with the formation of new solid phases, among which silver cyanide is predominant. © 1997 Academic Press

INTRODUCTION

Transition metal hexacyanoferrates exhibit a high sorption efficiency for several metallic ions in aqueous solutions. Caesium is one of these elements, whose sorption on such compounds is used for the decontamination of radioactive wastes (1–3). These hexacyanoferrates also exhibit a high affinity for silver ions. This property could be used for the removal of this expensive, but also toxic element from industrial wastes (4, 5). Silver also appears as a radioactive contaminant in the water of pressurized water reactors (6) and these compounds could be useful for its removal (3).

Development of decontamination methods requires a better knowledge of the sorption process. The word "sorption" as used here, is relative to any process involving the transfer of species dissolved in a solution to a solid immersed within this solution. A study of the sorption mechanisms of silver on nickel and zinc hexacyanoferrates (II) showed that the process strongly depends on the initial composition and crystal structure of the solid (7). The sorption process may be a phase transformation or a true ion exchange. These different mechanisms lead to different sorption kinetics, capacities, and stability of sorbent particles. In the case of potassium cobalt hexacyanoferrate (II), the sorption of silver seems to proceed with decomposition of the initial phase (8). Therefore, the choice of the most suitable compounds and experimental conditions for industrial applications will depend upon the mechanisms involved in the sorption.

In a systematic study devoted to the sorption of precious metals on several cyanocomplexes, it was observed that copper hexacyanoferrates are among the compounds that exhibit the highest sorption yields for silver (9). Therefore, we began a study on the sorption of silver on such copper- containing compounds. As shown in our previous studies (7), it is important to use a solid with well-defined composition and structure. In the case of copper hexacyanoferrates, several different solid phases exist (10, 11). The phases most often observed are cubic $Cu_2^{II}Fe^{II}(CN)_6\ xH_2O$ and $Cu_3^{II}[Fe^{III}\ (CN)_6]_2\ xH_2O$. Monoclinic $Na_2Cu^{II}Fe^{II}(CN)_6\ 10\,H_2O$ and triclinic $K_2Cu^{II}Fe^{II}(CN)_6$ were also observed.

The purpose of the present work is to study the sorption mechanisms of silver on $Cu_2^{II}Fe^{II}(CN)_6\ xH_2O$. This compound is prepared by precipitation in aqueous solution (11). A multidisciplinary approach was used to elucidate the sorption processes. Sorption kinetics, sorption isotherms, and capacity were determined by batch experiments. The balance of sorbed silver and of the constitutive elements released into the solution was systematically measured. Optical and electron microscopy, cyclic voltammetry, and X-ray diffraction were used in order to characterize the solid before and after silver sorption.

[1] To whom correspondence should be addressed.

0022-4596/97 $25.00

EXPERIMENTAL

Materials

The copper hexacyanoferrate was prepared by precipitation according to a method derived from Kawamura *et al.* (12): 0.125 *M* solutions of $Na_4Fe(CN)_6$ and $Cu(NO_3)_2$ were poured simultaneously in deionized water at 50°C, in order that the Cu/Fe ratio remained equal to 2.4. The precipitate was washed eight times with water by decantation and then filtered. It was dried in air at 30°C. It was then sieved under water flow in order to eliminate particles of size less than 25 μm, dried, crushed and, finally, sieved without water. Particle sizes between 25 and 71 μm were used in sorption experiments. This product is noted as Cu93.3B.

Chemical Analysis

Nondestructive neutron activation analyses (NAA) were performed for the determination of the elements Na, K, Cl, Cu, and Fe in the starting solid using the facilities of the Pierre Süe Laboratory. K and Cl were determined, since they may sometimes be found as impurities in the reagents used for the preparation of copper hexacyanoferrates (II), but were not detected in the present case. If we assume that one Fe atom is bound to six cyanide groups, the sum of the concentrations of Cu, Na, Fe, C, and N does not reach 100%. The difference to 100% was attributed to the presence of water. Thermogravimetric analysis (TGA) was also used for water content determination.

The starting solid was also analyzed for Na, K, Cu, and Fe by inductively coupled plasma atomic emission spectroscopy (ICPAES). For that purpose, 20-mg samples were dissolved into 10 ml of 11.6 *M* $HClO_4$ prior to analysis. ICPAES was also used for the analysis of the solutions after sorption experiments for Ag, Na, K, Cu, and Fe.

Batch Experiments

Fractions of 20 mg of the Cu93.3B compound were put into 20 ml of 0.1 *M* HNO_3 solutions containing known concentrations of silver. These fractions were mechanically shaken during a determined time in absence of light. In kinetic experiments, the initial silver concentration was constant in all solutions and equal to 4.4 Ag moles per mol of hexacyanoferrate (8.9×10^{-3} mol liter^{-1}), but the time of shaking varied from 5 min to 48 h. In sorption isotherm experiments, the shaking time was 48 h for all fractions, but the initial concentration in solutions varied from 0 to 6 Ag moles per mol of hexacyanoferrate (from 0 to 1.2×10^{-2} mol liter^{-1}). After shaking, the solid was filtered on a 0.2-μm porosity filter (mixed ester–cellulose ME24ST Schleicher and Schull filters). The filtrate was subjected to chemical analysis by ICPAES and the solid to optical and electron microscopy, X-ray diffraction, and cyclic voltammetry.

Optical and Scanning Electron Microscopy

Samples before and after silver sorption were observed by a binocular optical microscope with a magnification of 40. Samples were also deposited on aluminium plates and examined by a Zeiss DSM 950 scanning electron microscope under a voltage of 5 kV.

Cyclic Voltammetry

Fractions of 40 mg of powder were mixed with 160 mg of graphite (Lonka KS 44). Pellets were obtained under a pressure of about 1 kg cm^{-2} and introduced into an electrochemical cell described earlier (13). A saturated calomel electrode was used as a reference and a platinum wire as a counterelectrode. Several electrolytes were tested: 2 *M* H_2SO_4, 0.5 *M* K_2SO_4, 2 *M* HCl. The current was measured as a function of potential, with a scanning speed of 0.1 mV s^{-1} using a EGG PAR Programmer model 175 associated with a potentiostat model 363. Potential is referenced to the normal hydrogen electrode (NHE).

X-Ray Diffraction

A Siemens powder diffractometer D500 was used for crystal-structure studies. Identification of phases was conducted by reference to the ICDD database (release 1993). X-ray powder diffractions were simulated using Cerius software (release 1.5) from Molecular Simulations Inc.

RESULTS AND DISCUSSION

Composition, Structure, and Morphology of the Starting Copper Hexacyanoferrate (II)

The composition deduced from the chemical analysis is

$$Na_{0.028}Cu_{1.97}Fe(CN)_6\ 9.6\ H_2O.$$

This formulation is very close to the stoichiometric formula $Cu_2Fe(CN)_6\ xH_2O$. Such compound was identified by comparing X-ray powder diffraction patterns to literature data (ICDD 1.0244). It belongs to the cubic $Fm\bar{3}m$ ($z = 2 + 2/3$) structure. We then performed Rietveld refinement of diffraction data. A disordered structure was observed, with vacancies among iron sites. Copper occupies two types of sites, with vacancies in one of them. This structure will be described elsewhere in more details (14).

Optical and scanning electron microscopy showed that the solid is constituted of aggregates ranging between 20 and 70 μm, with irregular shapes and surfaces.

Silver Sorption Kinetics

The evolution of the composition of the solid phase expressed as the concentrations of silver and copper per iron as a function of the square root of time is shown in Fig. 1. The square root was chosen in order to expand the smallest time intervals. Two steps may be observed in the kinetics. The first step is a very quick process: within 5 min, almost all of the silver is transferred to the solid phase, and almost all of the copper is transferred to the solution. In the second step, a slow evolution of the solid is observed, with an increase of the silver content and a partial transfer of iron into the solution. As may be seen from these curves, the silver content rapidly exceeds 4 atoms per iron atom, thus indicating that the solid does not have the normal stoichiometry of hexacyanoferrates (II) or (III). At the same time, a nonnegligible part of iron is released into the solution which signifies a decomposition of the solid.

Silver Sorption Isotherm

The composition of the solid phase is shown in Fig. 2 as a function of the initial Ag/Fe ratio. In a first step, until approximately 4 atoms of silver per iron atom, the variation of the silver content in the solid is linear with a slope close to one, indicating an almost total fixation. The yield of sorption (Fig. 3, right scale) is greater than 99% until 3.7 Ag per Fe. For initial concentrations less than 0.01 mol liter^{-1}, this hexacyanoferrate is very efficient, since the yield of sorption is higher than 99.999%. As an example, for an initial silver concentration of 2×10^{-3} mol liter^{-1} the residual concentration is less than 2×10^{-8} mol liter^{-1}.

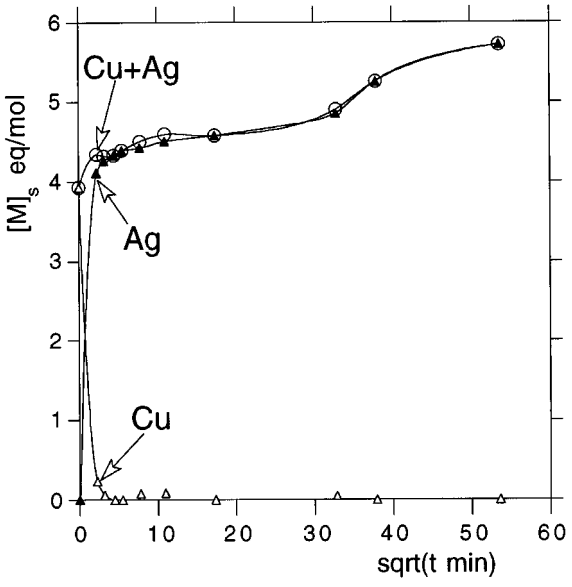

FIG. 1. Sorption kinetics of silver on $Cu_2Fe(CN)_6$ from 0.1 *M* HNO_3 solutions. Variation of the concentrations $[M]_s$ of silver, copper and the sum Ag + Cu in the solid in equivalents per iron atom as a function of the square root of time. The initial atomic Ag/Fe ratio is 4.4.

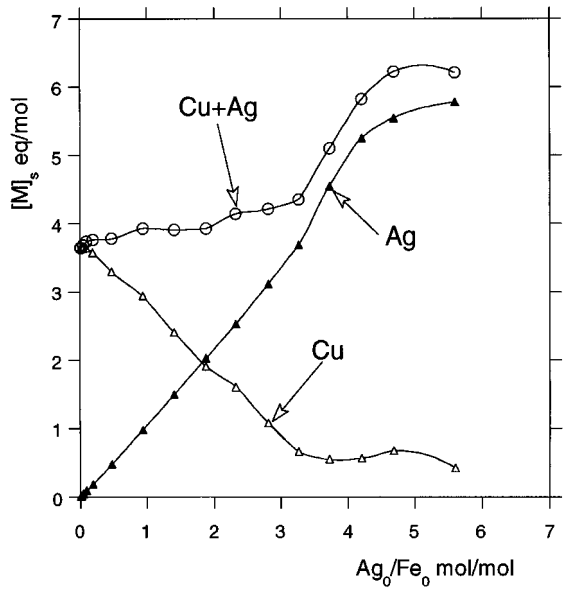

FIG. 2. Sorption isotherm of silver on $Cu_2Fe(CN)_6$ from 0.1 *M* HNO_3 solutions. Variation of the concentrations $[M]_s$ of silver, copper and the sum Ag + Cu in the solid in equivalents per iron atom as a function of the initial silver to iron ratio Ag_0/Fe_0.

After 4 Ag per Fe, the variation of the silver content (Fig. 2) is no longer linear, but it continues to increase and achieves values close to 6 Ag per Fe. The silver and the total cation contents both exceed the normal hexacyanoferrate stoichiometry.

The stoichiometry of the process may be seen from the variation of the dissolved copper to sorbed silver ratio (Fig. 3, left scale). For low silver contents (less than 1 Ag per Fe), this ratio is largely greater than one, indicating that more equivalents of copper are released from the solid into the solution than equivalents of silver are sorbed. This large ratio may be explained by a partial substitution of Cu^{2+} by H^+ in acid solutions, as it was proposed in the case of zinc hexacyanoferrates (7). Between 1 and 3 Ag per Fe, this ratio is close to one, which may correspond to a one to one equivalent exchange. Finally, above 3 Ag per Fe, there is more sorbed silver than removed copper.

As the sorption proceeds, some of the iron is released into the solution (Fig. 3, left scale) and reaches 27% for the highest silver concentration.

These observations indicate that this is not a simple ion exchange. A decomposition of the initial product and a phase transformation seem very likely. Complementary

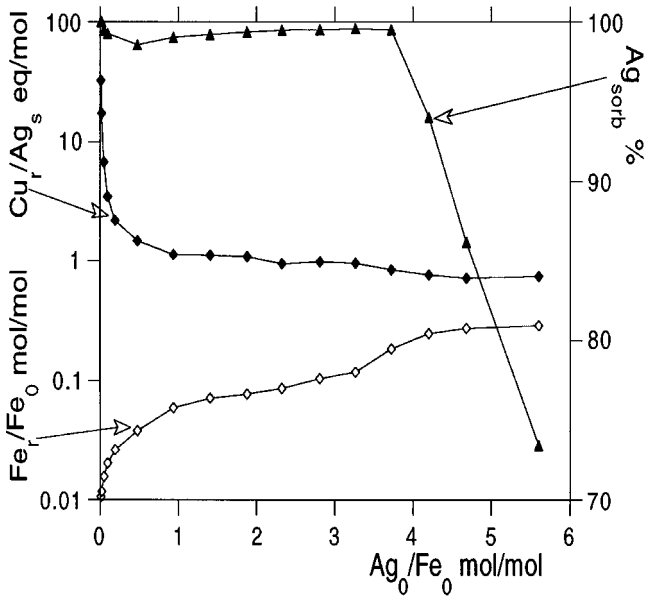

FIG. 3. Stoichiometry and yield of silver sorption on $Cu_2Fe(CN)_6$ from 0.1 *M* HNO_3 solutions. Variation of the ratio Cu_r/Ag_s of copper released into solution to silver sorbed into the solid, of the ratio Fe_r/Fe_0 of iron released into the solution to initial iron, and of the ratio of sorbed silver to initial silver (sorption yield or Ag_{sorb}) as a function of the initial silver to iron ratio Ag_0/Fe_0.

methods were therefore used in order to elucidate the mechanisms of the sorption process.

Optical and Scanning Electron Microscopy

Optical microscopy shows that for Ag/Fe ratios as low as 0.1, pink dots appear on the dark aggregates of copper hexacyanoferrate. For higher Ag/Fe ratios, the proportion of this pink precipitate increases. Scanning electron microscopy, shows that, at about 3 mol of Ag atom per Fe atom, a needle-shaped solid phase is observed (approximately 7 μm in length, 0.6 μm in diameter).

Cyclic Voltammetry

Copper, silver, and hexacyanoferrates can be electrochemically characterized since their standard potentials are within the electroactivity range of aqueous media. However, the electrochemical characterization of transition metal or silver cyanocompounds is carried out through a graphite powder electrode technique (13), because such solids have very low solubilities in aqueous solutions. In this case, the electrochemical reaction occurs at the interface between the graphite and solid particles. The soluble products are transferred to the liquid electrolyte.

Before proceeding with the solids used in this study, we performed measurements on some compounds with known compositions in order to acquire reference data. For that purpose we used copper (II) sulfate, silver cyanide, and potassium hexacyanoferrate (II). Then, measurements were performed with the copper hexacyanoferrate (II) Cu93-3B and the solids containing 1, 2, 3, 4, 5, and 6 silver atoms per iron atom, respectively. A sample assumed as a silver hexacyanoferrate (II) was precipitated by mixing solutions of potassium hexacyanoferrate (II) and silver nitrate and was also submitted to electrochemical measurements.

A summary of results is presented on Table 1. Examples of voltammograms are shown in Figs. 4–6.

The voltammogram of copper hexacyanoferrate (II) in 2 *M* H_2SO_4 shows two anodic peaks (A1 and A2) and two cathodic peaks (C1 and C2) (Fig. 4). Peak A1 and peak C1 appear at approximately 1.1 V NHE. They are observed in

TABLE 1
Summary of the Results Obtained by Cyclic Voltammetry on $Cu_2Fe(CN)_6$ before and after Silver Sorption and on Some Other Compounds

Compounds	Observed peaks A: anodic sweep C: cathodic sweep	Potential V NHE	Assignment
$Cu_2Fe(CN)_6$	A1, C1	1.1	Fe^{III}/Fe^{II} system
	A1′,C2′	1.2	
	C2	0.34	$Cu^{II} \rightarrow Cu^{I}$
	A2	0.66	$Cu^{I} \rightarrow Cu^{II}$
$Cu_2Fe(CN)_6$ + 1 Ag	A1, C1	0.9 to 1.1	Fe^{III}/Fe^{II} system
	C2	0.2	
	A2 (2nd cycle)	0.8	
$Cu_2Fe(CN)_6$ + 3 Ag	C1	0.9	
	C2 (1st cycle)	0.5 to 0.1	$AgCN \rightarrow Ag^0$
	C3 (2nd cycle)	0.3	
	A1	0.8	$Ag^0 \rightarrow Ag^+$
	A2	0.4	
$Cu_2Fe(CN)_6$ + 6 Ag	C1 (2nd cycle)	0.67	$Ag^+ \rightarrow Ag^0$
	C2, C2a, C2b	0.5 to 0.1	$AgCN \rightarrow Ag^0$
	A1 (2nd cycle)	0.77	$Ag^0 \rightarrow Ag^+$
	A2	0.54	$Ag^0 \rightarrow AgCN$
	A3	0.4	$Fe^{2+} \rightarrow Fe^{3+}$
AgCN	C1 (1st cycle)	0.4 to −0.05	$AgCN \rightarrow Ag^0$
	C2 (2nd cycle)	0.7 to 0.4	$Ag^+ \rightarrow Ag^0$
	C3 (2nd cycle)	0.4 to 0.1	$AgCN \rightarrow Ag^0$
	A1	0.84	$Ag^0 \rightarrow Ag^+$
	A2	0.53	$Ag^0 \rightarrow AgCN$
$Ag_4Fe(CN)_6$ (?)	C1 (2nd cycle)	0.65	$Ag^+ \rightarrow Ag^0$
	C2 (1st cycle)	0.4 to −0.1	$AgCN \rightarrow Ag^0$
	C3 (2nd cycle)	0.4 to 0.1	$AgCN \rightarrow Ag^0$
	A1 (2nd cycle)	0.8	$Ag^0 \rightarrow Ag^+$
	A2	0.4 to 0.6	$Ag^0 \rightarrow AgCN$
$K_4Fe(CN)_6$	A1	0.75	$Fe^{II} \rightarrow Fe^{III}$
	C1	0.4	
$CuSO_4$	C1	0.18	$Cu^{II} \rightarrow Cu^{I}$
	A1	0.5	$Cu^{I} \rightarrow Cu^{II}$

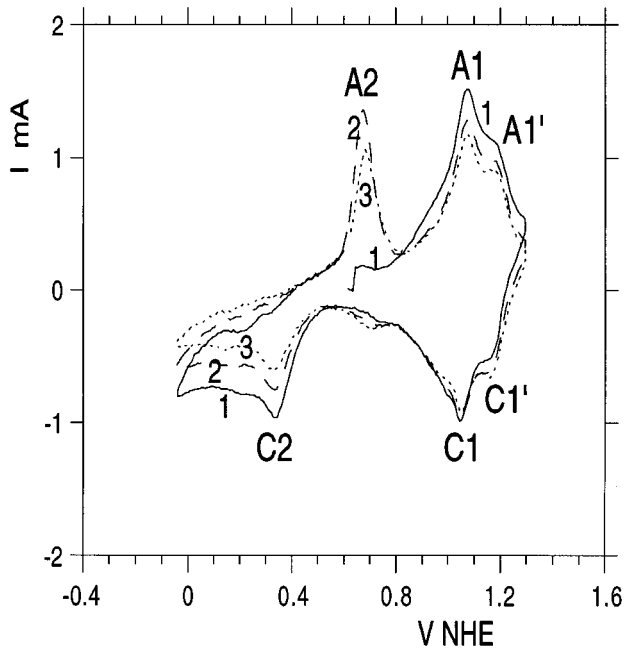

FIG. 4. Voltammogram of $Cu_2Fe(CN)_6$ in 2 *M* H_2SO_4. Variation of current *I* as a function of the potential *V* with reference to the normal hydrogen electrode. The cycle numbers are indicated on the curves.

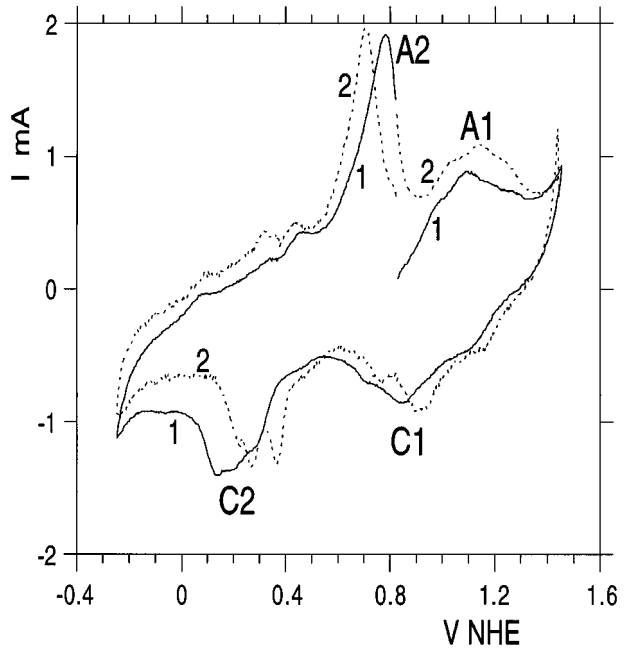

FIG. 5. Voltammogram of $Cu_2Fe(CN)_6$ with 1 mol silver per mol in 2 *M* H_2SO_4. Variation of current *I* as a function of the potential *V* with reference to the normal hydrogen electrode. The cycle numbers are indicated on the curves.

subsequent cycles. They belong to a fast and quasi-reversible electrochemical system and may be attributed to the Fe^{III}/Fe^{II} redox couple of the hexacyanoferrate. This peak couple can be identified as that already observed at approximately 1 V by several authors (15–17) on copper hexacyanoferrate films deposited on glassy carbon. Assigning this peak to the Fe^{III}/Fe^{II} couple was confirmed by Siperko *et al.* (15) using visible absorption spectrometry and X-ray photo-electron spectrometry (XPS). We note the presence of a couple of shoulders (A1′ and C1′) at approximately 1.2 V, but available data does not allow identification.

The cathodic peak C2 is observed in all cycles at approximately 0.34 V, whereas the anodic peak A2 at 0.66 V is observed from the second cycle onward. These peaks may be attributed to the Cu^{II}/Cu^{I} couple, the Cu^{I} state being formed during the cathodic sweep of the first cycle. Similar peaks were observed at respectively 0.25 and 0.60 V respectively by Siperko *et al.* (15).

We performed some comparisons with soluble salts. Potassium hexacyanoferrate (II) shows an anodic peak at 0.75 V and a cathodic peak at 0.4 V. No peaks are observed in subsequent cycles, indicating a diffusion of the salt out of the electrode. With the soluble copper sulfate, the cathodic peak appears at 0.18 V and the anodic peak at 0.50 V, indicating that, in hexacyanoferrates, the two corresponding peaks are shifted toward anodic regions.

In the presence of silver, even with the lowest concentrations of this element, the voltammograms are significantly modified. For one Ag mol per mol of copper hexacyanoferrate (Fig. 5), the peaks (A1, C1) corresponding to the Fe^{III}/Fe^{II} couple are highly attenuated; the cathodic peak (C2), previously observed near 0.34 V, is broadened and shifted toward the negative potentials, and an intense anodic peak (A2) appears at 0.8 V. In the second cycle, the peaks assigned to Fe^{II}/Fe^{III} are only slightly modified, the cathodic peak C2 is split into several peaks in the 0.2–0.3 V range and the intense anodic peak (A2) is shifted from 0.8 to 0.7 V.

With increasing silver concentration, the peaks assigned to Fe^{III}/Fe^{II} disappear for Ag/Fe ratios greater than 3 and new peaks appear. The voltammogram corresponding to 6 Ag per Fe is shown on Fig. 6, as an example. Three anodic peaks A1, A2 and A3 respectively at 0.77, 0.54 and 0.4 V are observed. An intense cathodic peak (C1) appears at 0.67 V; a broad cathodic peak (C2) with two shoulders (C2a, C2b) is observed in the 0.5–0.1 V range. The A1 and C1 peaks do not appear in the first cycle.

In the voltammograms obtained with silver cyanide, an intense anodic peak is observed at 0.84 V and a less intense peak at 0.53 V. For the cathodic sweep, an intense peak starting at approx. 0.4 V and with a maximum at 0.03 V is observed in the first cycle. During the second cycle, a broad cathodic peak ranging from 0.7 to 0.4 V appears, while the

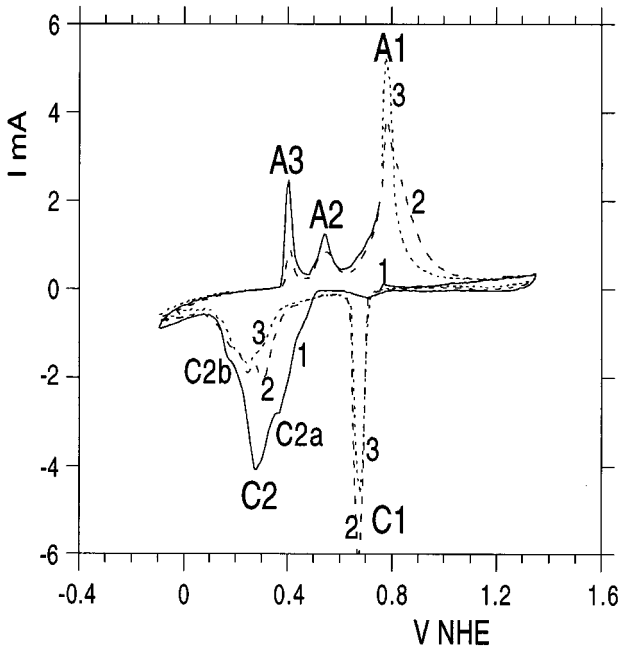

FIG. 6. Voltammogram of $Cu_2Fe(CN)_6$ with 6 mol silver per mol in 2 *M* H_2SO_4. Variation of current *I* as a function of the potential *V* with reference to the normal hydrogen electrode. The cycle numbers are indicated on the curves.

maximum of the cathodic peak observed in the first cycle is shifted toward 0.25 V and its intensity is attenuated.

With the assumed silver hexacyanoferrate, we observe an intense peak at 0.8 V during the anodic sweep, whose intensity increases from the first to the second cycle, and another peak, shifting from 0.52 V in the first cycle, to 0.44 V in the second cycle. During the cathodic sweep, we observe an intense peak at 0.65 V in the second and third cycles, and a broad system with several maxima ranging from 0.4 to -0.1 V in the first cycle, and from 0.4 to 0.1 V in the second cycle.

We have also considered the possibility of decomposition to iron hexacyanoferrate (Prussian Blue). Several measurements are reported for this compound in the literature (15, 18–21). Two peak couples, whose cathodic and anodic components have close potentials, were observed: one at 0.45 V and the other at 1.15 V.

The rapid disappearance of the Fe^{III}/Fe^{II} peaks, indicates that the initial hexacyanoferrate structure is destroyed even in the early stages of silver sorption. Such hexacyanoferrate structure does not exist in our assumed silver hexacyanoferrate, while it seems to be apparent in Prussian Blue, leading to the peak couple at 1.15 V. The second couple in Prussian Blue at 0.45 V may be assigned to the Fe^{3+}/Fe^{2+} system not coordinated to CN groups.

Voltammograms alone do not indicate equivocally the nature of the compounds resulting from the destruction of the initial hexacyanoferrate. However, it is possible to propose some compounds by comparing the voltammograms of hexacyanoferrates and reference compounds. The most probable compound seems to be silver cyanide and the observed voltammograms may be interpreted as follows: during the first cycle, the broad cathodic system (Fig. 6, C2, C2a, C2b at 0.5–0.1 V) may correspond to the reduction of silver in AgCN to Ag^0. Then, in the reversed scan, part of the previously formed silver is oxidized to AgCN (peak A2 at 0.54 V), while another part is oxidized to free Ag^+ (peak A1 at 0.77 V). In the second and third cycles, this "free" Ag^+ is reduced to Ag^0 (cathodic peak C1 at 0.67 V), but the intensity decreases due to diffusion into the solution. In the second and third cycles, the intensity of cathodic peaks assigned to AgCN is reduced due to a partial destruction of this compound. The anodic peak A3 at 0.4 V may be assigned to the oxidation of Fe^{2+} to Fe^{3+}, with diffusion into the solution. The possibility of the presence of Prussian Blue is not excluded, especially in the case of intermediate concentrations of silver (from 1 to 3 Ag per Fe). The presence of metallic silver is excluded since the peak corresponding to the oxidation of Ag^0 appears only after the first cathodic scan.

X-Ray Diffraction

The diffraction patterns of the starting copper hexacyanoferrate (II) of solids with increasing silver content and for silver cyanide are given in Table 2. The solids with the lowest silver content show the lines corresponding to cubic $Cu_2Fe(CN)_6\ xH_2O$. As the silver content increases, the line intensities of this phase decrease. A new phase appears, identified as rhombohedral silver cyanide (JCPDS-ICDD 23-1404). Finally, the $Cu_2Fe(CN)_6\ xH_2O$ phase disappears. For the highest silver concentrations, silver cyanide is dominant, but lines of another phase appear. This phase could not be identified and corresponds neither to any known silver compound, nor to metallic silver.

In the solids where the $Cu_2Fe(CN)_6\ xH_2O$ phase is still present, its unit-cell parameter decreases with increasing silver concentration.

Thus, X-ray diffraction measurements show that silver sorption induces the formation of new phases, mainly silver cyanide. Finally, the $Cu_2Fe(CN)_6\ xH_2O$ phase is completely destroyed, but the evolution of its parameter in the region where this phase is still present may indicate a partial substitution of copper by silver atoms.

Discussion

The first important result is that silver ions are removed with a high efficiency from the solution when they are put into contact with $Cu_2Fe(CN)_6$. As an example, from initial silver concentrations of 2×10^{-3} mol liter^{-1} (0.2 g liter^{-1}),

TABLE 2
Examples of X-Ray Diffraction Patterns of the Starting Solid $Cu_2Fe(CN)_6$, of Solids with Increasing Silver Content (Indicated as the Ag/Fe Ratio in the Solid), and for Silver Cyanide (ICDD 23.1014)

Ag/Fe:	0		0.11		1.15		5.1		AgCN	
a(Å):	9.991		9.962		0.971					
	d	*I*	*d*	*I*	*d*	*I*	*d*	*I*	*d*	*I*
	7.2173	26			6.4343	36	6.3555	15		
	5.7795	38	5.7343	31	5.7525	42	4.4689	5		
	4.9955	100	4.9720	100	4.9798	100	3.8309	9		
					3.6793	49	3.6690	33	3.669	45
	3.5329	90	3.5171	80	3.5225	87	3.5905	23		
	3.3398	38					3.4742	11		
	3.0075	36	2.9976	32	2.9927	64	3.3311	11		
			2.9666	27	2.6356	40	3.1748	12		
	2.4975	66	2.4892	55	2.4921	62	3.0467	15		
	2.2346	45	2.2259	38	2.2282	48	2.9818	100	3.001	100
	2.0395	39	2.0339	32	2.0341	39	2.5303	11		
			1.9175	24			2.3313	14	2.345	12
			1.7610	28	1.7632	37	2.3255	13	2.329	11
			1.6613	28	1.6618	37	2.3128	12		
			1.5762	28	1.5777	37	2.2554	9		
			1.5040	23			1.8726	8		
							1.8385	9	1.848	12
							1.8334	9	1.841	5
							1.7438	7		
							1.7262	11	1.733	8
									1.513	4
							1.4960	7	1.500	4

Note. *a*, lattice parameter for the cubic $Cu_2Fe(CN)_6$ phase (when present); *d*, reticular distance, *I*, relative intensity of diffraction lines.

the residual concentration is less than 2×10^{-8} mol liter^{-1} (2 μg liter^{-1}). This process has fast kinetics, since the main part of the transfer occurs in less than 5 min. The yield of retention is almost quantitative (close to 100%) until 4 moles per mol of solid. In a first approach, this last result and the one-to-one substitution of copper by silver in the solid phase could suggest an ion exchange process leading to $Ag_4Fe(CN)_6$. However, this process cannot be retained after further examination.

Sorption isotherms indicate that the transfer of silver to the solid phase is not a simple ion exchange. The sorption capacity reaches 6 Ag atoms per iron atom (1.4 g of Ag per g of hexacyanoferrate). This value exceeds the theoretical value of 4 atoms per atom. There is a progressive increase of the cations to iron ratio in the solid and a release of iron into the solution. The second step observed in kinetic experiments indicates a slow evolution of the solid after the initial fast fixation step.

The use of several complementary methods showed that silver sorption is a complex process. The main process is a progressive destruction of the initial structure, with the formation of new phases. It was clearly seen by optical microscopy. The main new phase is silver cyanide. The existence of this phase was proposed from the voltammetric experiments and confirmed by X-ray diffraction. This phase probably appears as needles in the scanning electron microscope observations. One or more other phases are also formed, but they were not identified. One of these phases may be Prussian Blue. The solid has a slightly blue color, but this compound was not detected by X-ray diffraction, because either its quantity was too small or it was not well crystallized. X-ray diffractions also showed that in the earliest stages some silver may be incorporated into the $Cu_2Fe(CN)_6$. The absence of Ag^0 in the first cycles of voltammetric experiments and in X-ray diffraction patterns excludes reduction to metallic silver during the sorption process.

Our studies also showed that the precipitate obtained by mixing solutions of potassium hexacyanoferrate (II) and silver nitrate is not a simple silver hexacyanoferrate (II) $Ag_4Fe(CN)_6$. This precipitates contains one or more phases, among which silver cyanide was identified. Finally, the existence of $Ag_4Fe(CN)_6$, suggested by Rock *et al.* (22), remains questionable. This compound may be an unstable intermediate state leading to silver cyanide.

Our present results may be compared with those found with other insoluble hexacyanoferrates. In our previous experiments (7) with zinc and nickel hexacyanoferrates (II),

we showed that for $Na_2Zn_3[Fe(CN)_6]_2$, in neutral pH solutions and for a Ag/Fe ratio less than 1, silver sorption proceeds with a real exchange with sodium ions, without alteration of the crystal structure. In contrast, for higher Ag/Fe ratios or for acid pH, one or more different solid phases are formed. A phase change always occurs when starting with other hexacyanoferrates: $Zn_2Fe(CN)_6$ or $Na_{2x}Ni_{2-x}Fe(CN)_6$. Silver cyanide was detected in the solid phase.

Sorption of silver was also studied on potassium–cobalt hexacyanoferrates (II) (4, 8). In the work of Lehto *et al.* (8), an ion exchange of silver with potassium is proposed in the early steps of the sorption, but it remains questionable, since other solid phases appear even at these steps. Large quantities of other phases appear in subsequent steps: among them silver cyanide was clearly identified as in our experiments.

CONCLUSION

If compared to other insoluble hexacyanoferrates, $Cu_2Fe(CN)_6$ is one of the best compounds for silver removal from solutions, especially for its high sorption capacity and fast kinetics. However, the sorption mechanisms are complex and several complementary techniques were necessary to acquire data on the main sorption processes. Ion exchange or surface complexation, usually proposed as the main processes in sorption phenomena, are not suitable in this case. A direct replacement of copper by silver in the initial structure does not occur or constitutes a minor process in the sorption. The main process is a destruction of the initial structure and the formation of new solid phases, among which silver cyanide is the main one. Further complementary techniques such as Mössbauer spectrometry or extended X-ray absorption fine structure spectroscopy (EXAFS) will be used to increase our knowledge of these mechanisms. However, the state of knowledge acquired through the present study is sufficient to predict some features of the experimental procedures for the use of insoluble hexacyanoferrates for decontamination purposes. $Cu_2Fe(CN)_6$ is certainly a very efficient sorbent for the removal of silver from aqueous solutions. However, its main use will be in batch procedures, instead of columns, since the phase transformation involved in the silver fixation will certainly destroy the initial solid particles and lead to clogging of the column. $Na_2Zn_3[Fe(CN)_6]_2$, in which an ion exchange process occurs, is certainly more favorable for column use, although in a more limited pH range and with a smaller sorption capacity. Further work must be done to define the experimental procedures that must be used for the decontamination of real liquid wastes.

REFERENCES

1. G. B. Barton, J. L. Helpworth, E. D. McClanahan Jr, R. L. Moore, and H. H. Van Tuyl, *Ind. Eng. Chem.* **50,** 212 (1958).
2. H. Loewenschuss, *Radioact. Waste Manage.* **2,** 327 (1982).
3. C. Loos-Neskovic and M. Fedoroff, *Radioact. Waste Manage.* **11**(2), 43 (1988).
4. M. Wald, W. Soyka, and B. Katsser, *Talanta* **20,** 405 (1973).
5. M. Fedoroff and C. Loos-Neskovic, *Mater. Tech.* 357 (1982).
6. M. Gavrilas and V. P. Guinn, *J. Radioanal. Nuclear Chem.* **113**(2), 327 (1987).
7. C. Loos-Neskovic and M. Fedoroff, *Solvent Extract. Ion Exchange* **5**(4), 757 (1987).
8. J. Lehto, S. Haukka, and M. Blomberg, *J. Solid State Chem.* **90,** 79 (1991).
9. M. Fedoroff, C. Loos-Neskovic, S. Abousahl, F. Adekola, J. C. Rouchaud, N. Boisseau, E. Garnier, E. Jackwerth, M. Dierkes, U. Rostek, and M. Kaeschagen, "Commission of European Communities, Summary Reports of the R&D Programme Recycling of Non-Ferrous Metals (1986–1989)," Contract MA1R1-0012-C (EDB), Report EUR 13646 EN, p. 145, 1992.
10. S. Ayrault, C. Loos-Neskovic, M. Fedoroff, and E. Garnier, *Talanta* **41,** 1435 (1994).
11. S. Ayrault, C. Loos-Neskovic, M. Fedoroff, E. Garnier, and D. Jones, *Talanta* **42,** 1581 (1995).
12. S. Kawamura, S. Shibata, K. Kurotaki, and H. Takeshita, *Anal. Chim. Acta* **102,** 225 (1978).
13. R. Vallot and L. T. Yu, *C. R. Acad. Sc. Paris* **284,** 759 (1977).
14. E. Garnier, D. Jones, C. Loos-Neskovic, and M. Fedoroff, in preparation.
15. L. M. Siperko and T. Kuwana, *J. Electrochem. Soc.* **130**(2), 396 (1983).
16. D. Engel and E. W. Grabner, *Ber. Bunsenges. Phys. Chem.* **89,** 982 (1985).
17. P. J. Kulesza and Z. Galus, *J. Electroanal. Chem.* **267,** 117 (1989).
18. B. J. Feldman and O. R. Melroy, *J. Electroanal. Chem.* **234,** 213 (1987).
19. S. Cowen, J. R. Sambles, and A. Glidle, *J. Electroanal. Chem.* **261,** 455 (1989).
20. H. Sugimura, N. Shimo, N. Kitamura and H. Masuhera, *J. Electroanal. Chem.* **346,** 147 (1993).
21. V. Plichon and S. Besbes, *Electrochim. Acta* **37,** 501 (1992).
22. P. A. Rock and R. E. Powell, *Inorg. Chem.* **15,** 1593 (1964).